MILCOM 2023 - 2023 IEEE Military Communications Conference (MILCOM) | 979-8-3503-2181-4/23/$31.00 ©2023 IEEE | DOI: 10.1109/MILCOM58377.2023.10356323

Machine Learning Based Node Selection for UWB Network Localization

Carlos A. Gómez-Vega*, Moe Z. Win†, and Andrea Conti*
*Department of Engineering and CNIT, University of Ferrara, Via Saragat 1, 44122 Ferrara, Italy
(e-mail: cgomez@ieee.org, a.conti@ieee.org)
†Laboratory for Information and Decision Systems, Massachusetts Institute of Technology, Cambridge, MA 02139 USA
(e-mail: moewin@mit.edu)

***Abstract*—In location-aware networks, only a subset of nodes provides representative measurements for position inference. Therefore, efficient high-accuracy localization calls for strategies to select an appropriate subset of active nodes. While node selection strategies benefit efficient localization, determining an optimal subset of active nodes relies on knowledge of channel state information whose acquisition overhead can be prohibitive. This paper presents a probabilistic node selection strategy for ultra-wideband network localization based on machine learning. We formulate the node selection problem as a classification task given a position estimate and determine near-optimal access probabilities from training data obtained via model-based optimization. A case study in a 3rd Generation Partnership Project scenario validates the proposed strategy and compares it against uniformly distributed random node selection.**

***Index Terms*—Localization, node selection, network operation, optimization, machine learning.**

I. Introduction

Location awareness [1] is essential for civil, industrial, and military applications including autonomy [2], public safety [3], and Internet-of-Things [4]. The 3rd Generation Partnership Project (3GPP) has defined performance requirements for seven positioning service levels in terms of accuracy, availability, and latency [5]. Location-aware networks must fulfill service-level requirements regardless of the operation conditions and employed technologies [6]. However, providing the required performance is difficult in complex wireless environments, especially under limited resources.

Location-aware networks consist of anchors with known positions and agents with unknown positions. Accurate localization depends on the wireless resources, propagation conditions, and deployment of nodes. In addition to localization algorithms [7]–[9], location-aware networks require strategies to optimize the utilization of wireless resources [10]. More specifically, network localization can benefit from strategies for the allocation of wireless resources [11], selection and coordination of active nodes [12], and deployment of nodes [13]. An appropriate selection of active nodes is crucial for efficient localization since only a subset of nodes provides representative measurements for position inference [14].

The problem of selecting representative measurements for inference tasks has been studied in various settings [15]–[19]. In location-aware networks, node selection strategies determine the subset of active nodes for inter-node measurements [20]–[24]. Conventional node selection strategies for localization rely on knowledge of position estimates and channel qualities to determine the optimal subset of nodes that minimizes the position error. While such strategies provide significant performance improvements, the acquisition of such parameters incurs signaling and processing overhead that can be prohibitive for location-based services with stringent latency requirements [5]. Probabilistic node selection reduces such an overhead by employing access probabilities to choose the active nodes [10]. However, the localization performance provided by probabilistic node selection relies on determining optimal access probabilities, which is challenging in complex wireless environments. In this regard, machine learning techniques [25]–[28] offer the possibility of estimating near-optimal access probabilities from training data.

The goal of this paper is to develop a probabilistic node selection strategy for efficient network localization in complex wireless environments. The key idea consists of formulating the node selection problem as a classification task to determine near-optimal access probabilities from training data.

This paper presents a probabilistic node selection strategy for network localization based on machine learning. We formulate the node selection problem as a classification task given a position estimate to learn access probabilities from training data obtained via model-based optimization. The key contributions of this paper are as follows:

- development of a probabilistic node selection strategy for network localization based on machine learning; and
- quantification of the performance provided by the developed node selection strategy.

The remaining sections are organized as follows: Section II formulates the problem. Section III describes the proposed node selection strategy. Section IV presents a case study. Finally, Section V gives our conclusions.

Notations: Random variables are displayed in sans serif, upright fonts; their realizations in serif, italic fonts. Vectors and matrices are denoted by bold lowercase and uppercase letters, respectively. For example, a variable is denoted by x; a random vector and its realization are denoted by x and $\boldsymbol{x}$, respectively; a matrix is denoted by $\boldsymbol{X}$. Sets are denoted by calligraphic font. For example, a set is denoted by $\mathcal{X}$. The m-dimensional vector of zeros (resp. ones) is denoted by $\mathbf{0}_m$

(resp. $\mathbf{1}_m$): the subscript is removed when the dimension of the vector is clear from the context. The transpose of a vector $\boldsymbol{x}$ is denoted by $\boldsymbol{x}^{\mathrm{T}}$. The trace of a matrix $\boldsymbol{X}$ is denoted by $\mathrm{tr}\{\boldsymbol{X}\}$. The Euclidean norm and direction of a vector $\boldsymbol{x}$ are denoted by $\|\boldsymbol{x}\|$ and $\angle\boldsymbol{x}$, respectively. Notation $\boldsymbol{a} \succcurlyeq \boldsymbol{b}$ denotes element-wise inequality between vectors $\boldsymbol{a}$ and $\boldsymbol{b}$.

II. Problem Formulation

This section formulates the node selection problem.

A. System Model

Consider a 2D location-aware network consisting of a single agent and N_{b} anchors with index set $\mathcal{N}_{\mathrm{b}} = \{1, 2, \ldots, N_{\mathrm{b}}\}$. The positions of the agent and anchor k are denoted by $\boldsymbol{p}$ and $\boldsymbol{p}_k$ for $k \in \mathcal{N}_{\mathrm{b}}$, respectively. The distance and angle between the positions of the agent and anchor k are denoted by $d_k(\boldsymbol{p}) = \|\boldsymbol{p} - \boldsymbol{p}_k\|$ and $\phi_k(\boldsymbol{p}) = \angle(\boldsymbol{p} - \boldsymbol{p}_k)$, respectively. The goal is to select a subset $\mathcal{N}_{\mathrm{s}} \subset \mathcal{N}_{\mathrm{b}}$ of $|\mathcal{N}_{\mathrm{s}}| = N_{\mathrm{s}}$ active anchors for inter-node measurements to maximally improve the localization accuracy of the agent.

The received waveform from anchor k at the agent is modeled as

$$r_k(t) = \sqrt{\gamma_k G} \sum_{l=1}^{L_k} \alpha_k^{(l)} s\big(t - \tau_k^{(l)}\big) + z_k(t) \tag{1}$$

where γ_k is the transmitting power, G is a gain related to the antenna directivity and center frequency, $s(t)$ is the transmitted waveform, L_k is the number of received multipath components, $\alpha_k^{(l)}$ and $\tau_k^{(l)}$ are the amplitude and delay of the lth received component, and $z_k(t)$ is the observation noise described by an additive white Gaussian process with two-sided power spectral density $N_0/2$. The channel coefficients are denoted by $\boldsymbol{w}_k = [\alpha_k^{(1)}, \tau_k^{(1)}, \alpha_k^{(2)}, \tau_k^{(2)}, \ldots, \alpha_k^{(L_k)}, \tau_k^{(L_k)}]^{\mathrm{T}}$, which is a realization of a random vector $\mathbf{w}_k$ with statistics according to a prescribed channel model [29], [30]. The relationship between the agent position and $\tau_k^{(l)}$ is given by

$$\tau_k^{(l)} = \frac{1}{c}\left[d_k(\boldsymbol{p}) + b_k^{(l)}\right] \tag{2}$$

where c is the propagation speed of the signal and $b_k^{(l)} \geqslant 0$ is a range bias with $b_k^{(1)} = 0$ and $b_k^{(1)} > 0$ for line-of-sight (LOS) and non-line-of-sight (NLOS) conditions, respectively [31].

B. Localization Performance Metric

The localization accuracy can be quantified in terms of the mean-square error (MSE) of the position estimator $\hat{\mathbf{p}}$ [32]. The equivalent Fisher information matrix (EFIM) for the agent position $\boldsymbol{p}$ as a function of the node selection vector (NSV) $\boldsymbol{u} = [u_1, u_2, \ldots, u_{N_{\mathrm{b}}}]^{\mathrm{T}}$ can be expressed as [14]

$$\boldsymbol{J}(\boldsymbol{u}; \boldsymbol{p}, \boldsymbol{w}, \boldsymbol{\gamma}) = \sum_{k=1}^{N_{\mathrm{b}}} u_k \, \xi_k(\boldsymbol{p}, \boldsymbol{w}_k, \gamma_k) \, \boldsymbol{J}_{\mathrm{r}}\big(\phi_k(\boldsymbol{p})\big) \tag{3}$$

where $u_k \in \{0, 1\}$ for $k \in \mathcal{N}_{\mathrm{b}}$, $\boldsymbol{w} = [\boldsymbol{w}_1^{\mathrm{T}}, \boldsymbol{w}_2^{\mathrm{T}}, \ldots, \boldsymbol{w}_{N_{\mathrm{b}}}^{\mathrm{T}}]^{\mathrm{T}}$, and $\boldsymbol{\gamma} = [\gamma_1, \gamma_2, \ldots, \gamma_{N_{\mathrm{b}}}]^{\mathrm{T}}$. In (3), $\xi_k(\boldsymbol{p}, \boldsymbol{w}_k, \gamma_k)$ is the range information intensity (RII) of the inter-node measurement with anchor k as a function of $\boldsymbol{p}$, $\boldsymbol{w}_k$, and γ_k, and $\boldsymbol{J}_{\mathrm{r}}(\phi)$ is the range direction matrix (RDM) with angle ϕ. The RII $\xi_k(\boldsymbol{p}, \boldsymbol{w}_k, \gamma_k)$ and RDM $\boldsymbol{J}_{\mathrm{r}}(\phi)$ are given by

$$\xi_k(\boldsymbol{p}, \boldsymbol{w}_k, \gamma_k) = \frac{8\pi^2\beta^2}{c^2}\big[1 - \chi_k(\boldsymbol{p}, \boldsymbol{w}_k)\big]\varrho_k(\boldsymbol{p}, \boldsymbol{w}_k, \gamma_k) \tag{4a}$$

$$\boldsymbol{J}_{\mathrm{r}}(\phi) = \begin{bmatrix} \cos^2\phi & \cos\phi\sin\phi \\ \cos\phi\sin\phi & \sin^2\phi \end{bmatrix} \tag{4b}$$

respectively. In (4a), β is the effective bandwidth of $s(t)$, $\chi_k(\boldsymbol{p}, \boldsymbol{w}_k) \in [0, 1)$ is the path-overlap coefficient (POC), and $\varrho_k(\boldsymbol{p}, \boldsymbol{w}_k, \gamma_k) = \gamma_k \, G \, (\alpha_k^{(1)})^2 / N_0$ is the signal-to-noise ratio (SNR) of the first received path.

The MSE of the position estimator $\hat{\mathbf{p}}$ as a function of the NSV $\boldsymbol{u}$ is lower bounded by [14]

$$\mathcal{P}(\boldsymbol{u}; \boldsymbol{p}, \boldsymbol{w}, \boldsymbol{\gamma}) = \mathrm{tr}\Big\{\big[\boldsymbol{J}(\boldsymbol{u}; \boldsymbol{p}, \boldsymbol{w}, \boldsymbol{\gamma})\big]^{-1}\Big\} \tag{5}$$

which is referred to as the squared position error bound (SPEB). This bound is asymptotically achievable and can be used for the design of node selection strategies [10].

C. Node Selection Problem

The goal of the node selection strategy is to minimize the position error by selecting N_{s} active anchors for inter-node measurements. Given knowledge of $\boldsymbol{p}$, $\boldsymbol{w}$, and $\boldsymbol{\gamma}$, the node selection problem can be formulated as

$$\mathscr{P}_{\boldsymbol{p},\boldsymbol{w},\boldsymbol{\gamma}}: \ \underset{\boldsymbol{u}}{\text{minimize}} \quad \mathcal{P}(\boldsymbol{u}; \boldsymbol{p}, \boldsymbol{w}, \boldsymbol{\gamma}) \tag{6a}$$

$$\text{subject to} \quad \boldsymbol{u}^{\mathrm{T}}\mathbf{1} = N_{\mathrm{s}} \tag{6b}$$

$$u_k \in \{0, 1\}, \quad k \in \mathcal{N}_{\mathrm{b}} \tag{6c}$$

where (6b) indicates the constraint on the total number of active anchors to be selected and (6c) describes the decision space of the variables in the NSV. The number of anchors N_{s} is a design choice that can also be optimized. The transmitting power levels can be set arbitrarily (e.g., uniform power allocation) or optimized via a node prioritization strategy [10]. Since $\mathcal{P}(\boldsymbol{u}; \boldsymbol{p}, \boldsymbol{w}, \boldsymbol{\gamma})$ is convex for $\boldsymbol{u} \succcurlyeq 0$ given $\boldsymbol{p}$, $\boldsymbol{w}$, and $\boldsymbol{\gamma}$, the combinatorial problem $\mathscr{P}_{\boldsymbol{p},\boldsymbol{w},\boldsymbol{\gamma}}$ can be solved approximately via a convex relaxation and a rounding operation [15], [33]. Specifically, the convex relaxation of (6) can be obtained by rewriting the constraint (6c) as $0 \leqslant u_k \leqslant 1$ for $k \in \mathcal{N}_{\mathrm{b}}$. Note that the optimal solution of the node selection problem (6) is lower bounded by that of its convex relaxation.

Remark 1: Solving (6) can be prohibitive for location-based services with stringent latency requirements due to the overhead of obtaining channel state information. This calls for strategies that do not require such a knowledge and select the active nodes based on probabilistic measures.

D. Probabilistic Node Selection

Probabilistic node selection is an alternative approach to solve (6) that reduces the overhead related to the acquisition of channel state information. In particular, this approach relies on a set of access probabilities $\mathcal{A}^{(\boldsymbol{p})} = \{p_1^{(\boldsymbol{p})}, p_2^{(\boldsymbol{p})}, \ldots, p_{N_{\mathrm{b}}}^{(\boldsymbol{p})}\}$ that depends on $\boldsymbol{p}$ with $p_k^{(\boldsymbol{p})} \geqslant 0$ and $\sum_{k=1}^{N_{\mathrm{b}}} p_k^{(\boldsymbol{p})} = 1$. Node selection strategies based on random access select anchors randomly according to predefined probabilities $p_k^{(\boldsymbol{p})}$, e.g., uniformly distributed random selection. Since such strategies can select any node with non-zero probability, the localization accuracy may be compromised with the overhead reduction. In contrast, node selection strategies based on deterministic access estimate access probabilities $\hat{p}_k^{(\boldsymbol{p})}$ and select the anchors with the highest scores. In the latter case, estimating optimal access probabilities is essential to obtain reliable localization performance. In the next section, we develop a probabilistic node selection strategy that estimates near-optimal access probabilities employing machine learning.

III. Probabilistic Node Selection Strategy

This section develops a probabilistic node selection strategy that learns access probabilities from training data.

A. Node Selection Strategy

Consider probabilistic node selection with optimized access probabilities $\mathring{\mathcal{A}}^{(\boldsymbol{p})} = \{\mathring{p}_1^{(\boldsymbol{p})}, \mathring{p}_2^{(\boldsymbol{p})}, \ldots, \mathring{p}_{N_\mathrm{b}}^{(\boldsymbol{p})}\}$ describing which of the available anchors are more likely to provide representative measurements to an agent located at $\boldsymbol{p}$. Given a position estimate $\hat{\boldsymbol{p}}$, we select the N_s anchors with the highest access probabilities. Therefore, we determine the NSV $\mathring{\boldsymbol{u}} = [\mathring{u}_1, \mathring{u}_2, \ldots, \mathring{u}_{N_\mathrm{b}}]^\mathrm{T}$ whose elements are given by

$$\mathring{u}_k = \begin{cases} 1 & \text{if } \mathring{p}_k^{(\hat{\boldsymbol{p}})} \text{ is one of the } N_\mathrm{s} \text{ largest elements in } \mathring{\mathcal{A}}^{(\hat{\boldsymbol{p}})} \\ 0 & \text{otherwise} \end{cases} \tag{7}$$

in which ties are broken arbitrarily. Fig. 1 illustrates this node selection strategy for $N_\mathrm{s} = 3$ active anchors. In this figure, clear-solid red annuluses represent anchors with low-high access probability, red-yellow contours depict the position uncertainty of the agent, and arrows denote the measurements with the active anchors selected. For optimized access probabilities, the localization performance provided by this strategy must approximate that obtained by solving $\mathscr{P}_{\boldsymbol{p},\boldsymbol{w},\boldsymbol{\gamma}}$, but without requiring any further parameter besides the position estimate. We propose a two-stage node selection strategy consisting of: (i) offline training to learn the access probabilities from data obtained via model-based optimization; and (ii) online operation to select the active anchors based on estimates of the probabilistic scores.

To determine the access probabilities, we consider a node prioritization problem for power allocation. The optimal solution to this problem provides information about how many and which anchors have to be selected for inter-node measurements as will be discussed next. Given $\boldsymbol{p}$ and $\boldsymbol{w}$, the considered node prioritization problem is formulated as

$$\breve{\mathscr{P}}_{\boldsymbol{p},\boldsymbol{w}}: \underset{\boldsymbol{\gamma}}{\text{minimize}} \quad \breve{\mathcal{P}}(\boldsymbol{\gamma}; \boldsymbol{p}, \boldsymbol{w}) \tag{8a}$$

$$\text{subject to} \quad \boldsymbol{\gamma}^\mathrm{T}\mathbf{1} \leqslant \gamma_\mathrm{T} \tag{8b}$$

$$\boldsymbol{\gamma} \succcurlyeq \mathbf{0} \tag{8c}$$

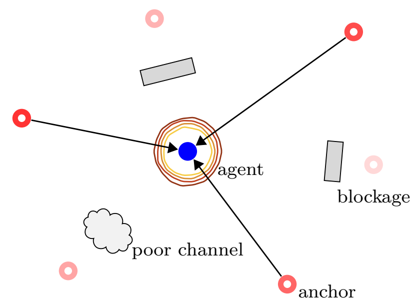

Fig. 1. Probabilistic node selection strategy: anchors are selected based on access probabilities given a position estimate.

where the EFIM for the agent position $\boldsymbol{p}$ and SPEB are rewritten as functions of the vector $\boldsymbol{\gamma}$ as

$$\breve{\boldsymbol{J}}(\boldsymbol{\gamma}; \boldsymbol{p}, \boldsymbol{w}) = \sum_{k=1}^{N_\mathrm{b}} \xi_k(\boldsymbol{p}, \boldsymbol{w}_k, \gamma_k)\, \boldsymbol{J}_\mathrm{r}\big(\phi_k(\boldsymbol{p})\big) \tag{9a}$$

$$\breve{\mathcal{P}}(\boldsymbol{\gamma}; \boldsymbol{p}, \boldsymbol{w}) = \mathrm{tr}\Big\{\big[\breve{\boldsymbol{J}}(\boldsymbol{\gamma}; \boldsymbol{p}, \boldsymbol{w})\big]^{-1}\Big\} \tag{9b}$$

respectively. In $\breve{\mathscr{P}}_{\boldsymbol{p},\boldsymbol{w}}$, (8b) indicates the constraint on the total transmitting power γ_T and (8c) describes that the transmitting power levels are nonnegative. The objective in (8a) is convex for $\boldsymbol{\gamma} \succcurlyeq \mathbf{0}$ given $\boldsymbol{p}$ and $\boldsymbol{w}$ [10]. Therefore, $\breve{\mathscr{P}}_{\boldsymbol{p},\boldsymbol{w}}$ is a convex program that can be solved via standard convex optimization techniques, e.g., interior-point methods [33]. Note that the problem $\breve{\mathscr{P}}_{\boldsymbol{p},\boldsymbol{w}}$ can be transformed into a second-order cone program (SOCP) allowing the use of efficient solvers [10].

Let $\breve{\boldsymbol{\gamma}} = [\breve{\gamma}_1, \breve{\gamma}_2, \ldots, \breve{\gamma}_{N_\mathrm{b}}]^\mathrm{T}$ denote the optimal solution to (8). Such a solution can be used to determine both the number of active anchors and the NSV simultaneously. More specifically, the optimal NSV related to $\breve{\boldsymbol{\gamma}}$ is denoted by $\breve{\boldsymbol{u}} = [\breve{u}_1, \breve{u}_2, \ldots, \breve{u}_{N_\mathrm{b}}]^\mathrm{T}$ with elements given as

$$\breve{u}_k = \begin{cases} 1 & \text{if } \breve{\gamma}_k > 0 \\ 0 & \text{otherwise} \end{cases} \tag{10}$$

and the optimal number of active anchors is $\breve{N}_\mathrm{s} = \breve{\boldsymbol{u}}^\mathrm{T}\mathbf{1}$. The sparsity property of $\breve{\boldsymbol{\gamma}}$ establishes that the transmitting resources are allocated to at most three active anchors [10]. Therefore, we have that $\breve{N}_\mathrm{s} \leqslant 3$. In particular, we employ NSVs in the form of $\breve{\boldsymbol{u}}$ to obtain training data for learning near-optimal access probabilities via machine learning.

B. Training Phase

Consider a classification problem where, given a position estimate $\hat{\boldsymbol{p}}$, we determine a vector of access probabilities $\hat{\boldsymbol{a}} = [\hat{p}_1, \hat{p}_2, \ldots, \hat{p}_{N_\mathrm{b}}]^\mathrm{T}$ for soft node selection based on (7). Such a problem consists of N_b classes each of which representing the selection of a single anchor. The goal is to determine a parametric mapping to estimate the access probabilities in a supervised learning setting with training data obtained from solving instantiations of the problem $\breve{\mathscr{P}}_{\boldsymbol{p},\boldsymbol{w}}$. For a given instantiation of $\breve{\mathscr{P}}_{\boldsymbol{p},\boldsymbol{w}}$, we break the optimal NSV

Algorithm 1 Training phase

Output: Approximate mapping $f(\,\cdot\,; \mathring{\boldsymbol{\psi}})$.

1: Acquire training data $\{\hat{\boldsymbol{p}}^{(m)}, \breve{\boldsymbol{s}}^{(m)}\}_{m\in\mathcal{N}_{\text{train}}}$:
   Obtain position estimate $\hat{\boldsymbol{p}}$;
   Solve the model-based node prioritization problem (8);
   Determine the NSV $\breve{\boldsymbol{u}}$ with elements given by (10); and
   Break NSV $\breve{\boldsymbol{u}}$ into one-hot encoded vectors.

2: Determine approximate mapping $f(\,\cdot\,; \mathring{\boldsymbol{\psi}})$ by fitting the parameters of a prescribed neural network architecture to training data.

$\breve{\boldsymbol{u}}$ into $\breve{N}_{\text{s}}$ vectors indicating the selection of a single anchor using one-hot encoding (also referred as 1-of-K encoding for K classes [27]). Let $\boldsymbol{s}^{(i)} = [\,s_1^{(i)}, s_2^{(i)}, \ldots, s_{N_{\text{b}}}^{(i)}]^{\text{T}}$ denote the one-hot encoded vector for the selection of anchor i whose elements are given by

$$s_k^{(i)} = \begin{cases} 1 & \text{if } i = k \\ 0 & \text{otherwise} \end{cases} \tag{11}$$

for $k \in \mathcal{N}_{\text{b}}$. Therefore, each instantiation of the problem $\breve{\mathscr{P}}_{\boldsymbol{p},\boldsymbol{w}}$ with solution $\breve{\boldsymbol{u}}$ provides $\breve{N}_{\text{s}}$ training examples of the form $(\hat{\boldsymbol{p}}, \boldsymbol{s}^{(k)})$ for k such that $\breve{u}_k = 1$.

Let $\mathcal{X}$ and $\mathcal{A}$ denote the state and decision spaces, respectively, such that $\hat{\boldsymbol{p}} \in \mathcal{X}$ and $\hat{\boldsymbol{a}} \in \mathcal{A}$. We consider a mapping $f : \mathcal{X} \mapsto \mathcal{A}$ that provides near-optimal access probabilities for node selection given position estimates. Let $\mathcal{F}$ denote a parametric family of mappings with parameter space $\mathit{\Psi}$. Each $\boldsymbol{\psi} \in \mathit{\Psi}$ determines a different mapping $f(\,\cdot\,; \boldsymbol{\psi}) \in \mathcal{F}$. Specifically, we consider a neural network architecture to obtain the desired mapping for probabilistic node selection. In the training phase, we determine the parameters $\mathring{\boldsymbol{\psi}} \in \mathit{\Psi}$ of the prescribed neural network architecture that provide the best fit to training data [34], [35]. Let $\{\hat{\boldsymbol{p}}^{(m)}, \breve{\boldsymbol{s}}^{(m)}\}_{m\in\mathcal{N}_{\text{train}}}$ denote the training data indexed by $\mathcal{N}_{\text{train}}$. The position estimate can be obtained using a specific localization algorithm, and the target vector corresponds to one-hot encoded single anchor selection obtained from model-based optimization in (8). In particular, the model-based node prioritization problem can be solved by transforming it into an SOCP and using a standard interior-point method. For classification problems, the output layer of the neural network employs a softmax activation function that enables the probabilistic interpretation of a categorical distribution with N_{b} elements, and the objective function to fit the model is the cross entropy loss [27], [28]. By minimizing the cross entropy loss in the training phase, the neural network is encouraged to match the labels of the training data and approximate the desired distribution [35]. Algorithm 1 describes the training phase of the proposed strategy.

C. Operation Phase

The training phase determines the parametric mapping $f(\,\cdot\,, \mathring{\boldsymbol{\psi}})$ to estimate access probabilities for online node selection. In the online phase, we rely on a position estimate

Algorithm 2 Online node selection

Input: Position estimate $\hat{\boldsymbol{p}}$, number of active anchors N_{s}.

Output: NSV $\hat{\boldsymbol{u}}$.

1: Estimate access probabilities using the approximate mapping obtained in the training phase
   $\hat{\boldsymbol{a}} \leftarrow f(\hat{\boldsymbol{p}}; \mathring{\boldsymbol{\psi}})$.

2: Determine $\hat{\boldsymbol{u}}$ by evaluating (13) based on $\hat{\boldsymbol{a}}$ and N_{s}.

to determine the access probabilities and perform the node selection. Given a position estimate $\hat{\boldsymbol{p}}$, we obtain the access probabilities by evaluating the parametric mapping of the feed-forward neural network as

$$\hat{\boldsymbol{a}} = f(\hat{\boldsymbol{p}}; \mathring{\boldsymbol{\psi}})\,. \tag{12}$$

Then, we select N_{s} anchors according to the estimated NSV $\hat{\boldsymbol{u}} = [\,\hat{u}_1, \hat{u}_2, \ldots, \hat{u}_{N_{\text{b}}}]^{\text{T}}$ with elements given by

$$\hat{u}_k = \begin{cases} 1 & \text{if } \hat{p}_k \text{ is one of the } N_{\text{s}} \text{ largest elements in } \hat{\boldsymbol{a}} \\ 0 & \text{otherwise} \end{cases} \tag{13}$$

in which ties are broken arbitrarily. In particular, the number of active anchors N_{s} can be used as an input to provide further degrees of freedom. Algorithm 2 describes the operation of the proposed node selection strategy in the online phase.

IV. Case Study

This section validates the proposed node selection strategy in a case study. We consider ultra-wideband (UWB) nodes [36] emitting root raised cosine pulses compliant with the IEEE 802.15.4a standard [37]. The anchors are deployed according to the 3GPP indoor open office scenario with $N_{\text{b}} = 12$ (see Fig. 2) [30]. The wireless channels are modeled according to the IEEE 802.15.4a channel model for the indoor office scenario [29]. We consider spatially-consistent LOS/NLOS states and wireless channel coefficients [38] with the parameters specified for the 3GPP indoor open office scenario in [30]. The RII between nodes in LOS and NLOS conditions are determined following [39] and set to zero, respectively. The noise figure, center frequency, and maximum power spectral density are 10 dB, 6.489 GHz, and -41.3 dBm/MHz, respectively [37]. The training data is generated by solving 10,000 instantiations of the node prioritization problem with random agent positions using CVX [40]. We consider 70% of the data for training and 30% for validation. The localization performance is evaluated on new instantiations of test data that are not included in the training phase.

We consider a fully-connected neural network architecture consisting of three hidden layers with 64, 128, and 16 neurons, respectively, to validate the proposed approach. The input and output layers have sizes of 2 and 12, respectively. The activation functions of the hidden layers are rectified linear units. The activation functions of the output layer are

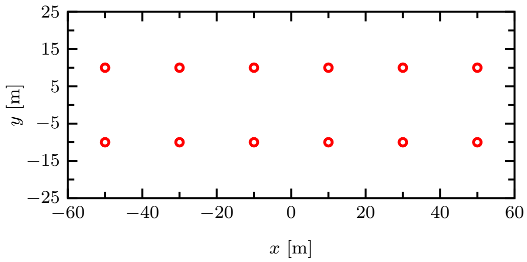

Fig. 2. Anchor deployment for the 3GPP indoor open office scenario [30].

softmax functions. The neural networks are trained using the Adam algorithm [28] with 30 epochs and batch size of 128.

Table I shows the results of the training phase on validation data for different values of N_s. We consider the accuracy metric as the percentage of cases in which the anchors selected by model-based optimization with perfect knowledge of the channel state information are included in the set of anchors chosen by the proposed strategy. The table also reports the percentage of active anchors in LOS and NLOS conditions, respectively. We can observe that, as N_s increases, it is more likely to select the anchors with the most favorable conditions as dictated by the solutions to the node prioritization problem. However, the percentage of anchors in LOS conditions decreases as N_s grows, indicating that more nodes in unfavorable conditions are chosen. In particular, these results show that neural networks can effectively learn from the environment to provide reliable access probabilities for node selection. Note that the proposed node selection strategy only relies on an estimate of the agent position, while model-based optimization requires channel state information of every anchor to provide desirable performance.

Table II shows the results of the operation phase on test data for different values of N_s considering the same metrics above. The test data used for this evaluation was not included in the training phase. The results for online operation are consistent with those obtained during training. We can observe that the accuracy improves, while the percentage of active anchors in LOS and NLOS conditions are similar to those obtained in the training phase. These results indicate the effective training of the neural network for reliable online operation.

Next, we evaluate the performance provided by the trained neural network in online operation. We compare the following strategies considering uniform power allocation:

- uniformly distributed random node selection — N_s active anchors in LOS conditions are selected randomly according to a uniform distribution;
- probabilistic node selection — N_s active anchors are selected according to the proposed node selection strategy.

In particular, localization performance is evaluated in terms of the empirical cumulative distribution function (ECDF) of the position error metric (the square root of the SPEB).

Fig. 3 shows the performance of the proposed node selection strategy for different values of N_s. We consider the performance obtained via model-based optimization with perfect knowledge of channel state information as benchmark. We can observe that the proposed node selection strategy outperforms conventional strategies based on uniformly distributed random selection. Note that, for $N_s = 3$ active anchors, the performance approaches that obtained via model-based optimization with optimal power allocation. Note that the gaps with respect to the benchmark are due to the absence of channel state information and the use of uniform power allocation. For example, the position errors of the proposed node prioritization strategy with $N_s = 3$ and the model-based optimization at the 80th percentile are 0.81 and 0.66 m, respectively, implying a performance loss of 22.7%. At such mark, random node selection with $N_s = 3$ provides an error of 2.29 m, implying that the proposed strategy reduces the position error by 64.6%. The results indicate that the proposed node selection strategy can select favorable anchors and provide adequate performance with only the position estimate as parameter.

TABLE I
TRAINING PHASE RESULTS ON VALIDATION DATA.

N_s	Accuracy (%)	LOS (%)	NLOS (%)
3	74.8	89.2	10.8
4	90.0	84.1	15.9
5	95.5	77.5	22.5
6	98.4	71.9	28.1

TABLE II
OPERATION PHASE RESULTS ON TEST DATA.

N_s	Accuracy (%)	LOS (%)	NLOS (%)
3	77.8	89.0	11.0
4	91.3	84.0	16.0
5	96.3	77.6	22.4
6	98.7	71.9	28.1

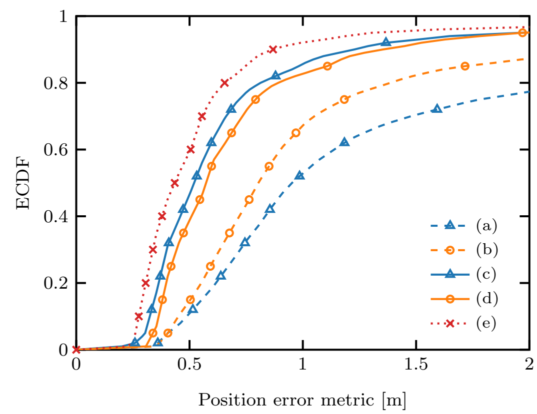

Fig. 3. ECDF of the position error metric for: (a) uniformly distributed random selection with $N_s = 3$; (b) uniformly distributed random selection with $N_s = 4$; (c) proposed strategy with $N_s = 3$; (d) proposed strategy with $N_s = 4$; and (e) model-based optimization.

V. CONCLUSION

This paper presented a probabilistic node selection strategy for UWB network localization based on machine learning. Specifically, the node selection problem is formulated as a classification task to learn near-optimal access probabilities from training data obtained via model-based optimization. Numerical results in a 3GPP indoor open office scenario show the benefits of probabilistic node selection for efficient localization. In particular, the trained neural network learns from the environment and allows selecting the active anchors with only an estimate of the agent position. The proposed node selection strategy shows the effectiveness of machine learning techniques to optimize the operation of location-aware networks in complex wireless environments.

Acknowledgment

The fundamental research described in this paper was supported, in part, by the Office of Naval Research under Grant N62909-22-1-2009, by the National Science Foundation under Grant CNS-2148251, and by federal agency and industry partners in the RINGS program.

References

[1] M. Z. Win *et al.*, "Network localization and navigation via cooperation," *IEEE Commun. Mag.*, vol. 49, no. 5, pp. 56–62, May 2011.

[2] A. Guerra, F. Guidi, D. Dardari, and P. M. Djurić, "Networks of UAVs of low complexity for time-critical localization," *IEEE Aerosp. Electron. Syst. Mag.*, vol. 37, no. 10, pp. 22–38, Oct. 2022.

[3] A. R. Ansari, N. Saeed, M. I. Ul Haq, and S. Cho, "Accurate 3D localization method for public safety applications in vehicular ad-hoc networks," *IEEE Access*, vol. 6, pp. 20 756–20 763, 2018.

[4] L. Chen *et al.*, "Robustness, security and privacy in location-based services for future IoT: A survey," *IEEE Access*, vol. 5, pp. 8956–8977, Apr. 2017.

[5] *Technical Specification Group Services and System Aspects; Service requirements for the 5G system; Stage 1*, 3rd Generation Partnership Project 3GPP™ TS 22.261 V18.6.0 (2022-03), Mar. 2022, Release 18.

[6] A. Conti *et al.*, "Location awareness in beyond 5G networks," *IEEE Commun. Mag.*, vol. 59, no. 11, pp. 22–27, Nov. 2021, special issue on *Location Awareness for 5G and Beyond*.

[7] X. Wang, X. Wang, and S. Mao, "Deep convolutional neural networks for indoor localization with CSI images," *IEEE Trans. Netw. Sci. Eng.*, vol. 7, no. 1, pp. 316–327, Jan.-Mar. 2020.

[8] F. Morselli, S. M. Razavi, M. Z. Win, and A. Conti, "Soft information based localization for 5G networks and beyond," *IEEE Trans. Wireless Commun.*, vol. 22, pp. 1–16, 2023, to appear.

[9] S. Safavi, U. A. Khan, S. Kar, and J. M. F. Moura, "Distributed localization: A linear theory," *Proc. IEEE*, vol. 106, no. 7, pp. 1204–1223, Jul. 2018.

[10] M. Z. Win, W. Dai, Y. Shen, G. Chrisikos, and H. V. Poor, "Network operation strategies for efficient localization and navigation," *Proc. IEEE*, vol. 106, no. 7, pp. 1224–1254, Jul. 2018, special issue on *Foundations and Trends in Localization Technologies*.

[11] H. Godrich, A. P. Petropulu, and H. V. Poor, "Power allocation strategies for target localization in distributed multiple-radar architectures," *IEEE Trans. Signal Process.*, vol. 59, no. 7, pp. 3226–3240, Jul. 2011.

[12] T. Wang, Y. Shen, A. Conti, and M. Z. Win, "Network navigation with scheduling: Error evolution," *IEEE Trans. Inf. Theory*, vol. 63, no. 11, pp. 7509–7534, Nov. 2017.

[13] J. J. Khalife and Z. M. Kassas, "Optimal sensor placement for dilution of precision minimization via quadratically constrained fractional programming," *IEEE Trans. Aerosp. Electron. Syst.*, vol. 55, no. 4, pp. 2086–2096, Aug. 2019.

[14] M. Z. Win, Y. Shen, and W. Dai, "A theoretical foundation of network localization and navigation," *Proc. IEEE*, vol. 106, no. 7, pp. 1136–1165, Jul. 2018, special issue on *Foundations and Trends in Localization Technologies*.

[15] S. Joshi and S. Boyd, "Sensor selection via convex optimization," *IEEE Trans. Signal Process.*, vol. 57, no. 2, pp. 451–462, Feb. 2009.

[16] S. Bartoletti, A. Giorgetti, M. Z. Win, and A. Conti, "Blind selection of representative observations for sensor radar networks," *IEEE Trans. Veh. Technol.*, vol. 64, no. 4, pp. 1388–1400, Apr. 2015.

[17] X. Shen, S. Liu, and P. K. Varshney, "Sensor selection for nonlinear systems in large sensor networks," *IEEE Trans. Aerosp. Electron. Syst.*, vol. 50, no. 4, pp. 2664–2678, Oct. 2014.

[18] G. Torsoli, M. Z. Win, and A. Conti, "Selection of reference base station for TDOA-based localization in 5G and beyond IIoT," in *Proc. IEEE Global Telecomm. Conf.*, Rio de Janeiro, Brazil, Dec. 2022, pp. 317–322.

[19] V. Gupta, T. H. Chung, B. Hassibi, and R. M. Murray, "On a stochastic sensor selection algorithm with applications in sensor scheduling and sensor coverage," *Automatica*, vol. 42, no. 2, pp. 251–260, 2006.

[20] X. Li, N. Mitton, I. Simplot-Ryl, and D. Simplot-Ryl, "Dynamic beacon mobility scheduling for sensor localization," *IEEE Trans. Parallel Distrib. Syst.*, vol. 23, no. 8, pp. 1439–1452, Aug. 2012.

[21] S. Dwivedi, D. Zachariah, A. De Angelis, and P. Händel, "Cooperative decentralized localization using scheduled wireless transmissions," *IEEE Commun. Lett.*, vol. 17, no. 6, pp. 1240–1243, Jun. 2013.

[22] X. Shen and P. K. Varshney, "Sensor selection based on generalized information gain for target tracking in large sensor networks," *IEEE Trans. Signal Process.*, vol. 62, no. 2, pp. 363–375, Jan. 2014.

[23] L. Song, T. Zhang, X. Yu, C. Qin, and Q. Zhang, "Scheduling in cooperative UWB localization networks using round trip measurements," *IEEE Commun. Lett.*, vol. 20, no. 7, pp. 1409–1412, Jul. 2016.

[24] T. Wang, A. Conti, and M. Z. Win, "Network navigation with scheduling: Distributed algorithms," *IEEE/ACM Trans. Netw.*, vol. 27, no. 4, pp. 1319–1329, Aug. 2019.

[25] A. Zappone, M. D. Renzo, and M. Debbah, "Wireless networks design in the era of deep learning: Model-based, AI-based, or both?" *IEEE Trans. Commun.*, vol. 67, no. 10, pp. 7331–7376, Oct. 2019.

[26] Y. C. Eldar, A. Goldsmith, D. Gündüz, and H. V. Poor, *Machine Learning and Wireless Communications*. New York, NY: Cambridge University Press, 2022.

[27] C. M. Bishop, *Pattern Recognition and Machine Learning*. New York, NY, USA: Springer, 2006.

[28] I. Goodfellow, Y. Bengio, and A. Courville, *Deep Learning*. Cambridge, MA: MIT Press, 2017. [Online]. Available: http://www.deeplearningbook.org

[29] A. F. Molisch *et al.*, "A comprehensive standardized model for ultrawideband propagation channels," *IEEE Trans. Antennas Propag.*, vol. 54, no. 11, pp. 3151–3166, Nov. 2006, special issue on *Wireless Communications*.

[30] *Technical Specification Group Radio Access Network; Study on channel model for frequencies from 0.5 to 100 GHz*, 3rd Generation Partnership Project 3GPP™ 3GPP TR 38.901 V16.1.0 (2019-12), Dec. 2019, Release 16.

[31] A. Conti, M. Guerra, D. Dardari, N. Decarli, and M. Z. Win, "Network experimentation for cooperative localization," *IEEE J. Sel. Areas Commun.*, vol. 30, no. 2, pp. 467–475, Feb. 2012.

[32] H. L. Van Trees, *Detection, Estimation, and Modulation Theory*, 1st ed. New York, NY 10158-0012: John Wiley & Sons, Inc., 1968.

[33] S. Boyd and L. Vandenberghe, *Convex Optimization*. Cambridge, UK: Cambridge University Press, 2004.

[34] N. Shlezinger, Y. C. Eldar, and S. P. Boyd, "Model-based deep learning: On the intersection of deep learning and optimization," *IEEE Access*, vol. 10, pp. 115 384–115 398, 2022.

[35] N. Shlezinger, J. Whang, Y. C. Eldar, and A. G. Dimakis, "Model-based deep learning," *Proc. IEEE*, vol. 111, no. 5, pp. 465–499, May 2023.

[36] M. Z. Win and R. A. Scholtz, "Impulse radio: How it works," *IEEE Commun. Lett.*, vol. 2, no. 2, pp. 36–38, Feb. 1998.

[37] "IEEE standard for information technology - telecommunications and information exchange between systems - local and metropolitan area networks - specific requirement part 15.4: Wireless medium access control (MAC) and physical layer (PHY) specifications for low-rate wireless personal area networks (WPANs)," *IEEE Std 802.15.4a-2007 (Amendment to IEEE Std 802.15.4-2006)*, pp. 1–203, 2007.

[38] F. Ademaj, S. Schwarz, T. Berisha, and M. Rupp, "A spatial consistency model for geometry-based stochastic channels," *IEEE Access*, vol. 7, pp. 183 414–183 427, 2019.

[39] C. A. Gómez-Vega, F. Morselli, M. Z. Win, and A. Conti, "A statistical range information model with application to UWB localization," in *Proc. Military Commun. Conf.*, San Diego, CA, Nov. 2021, pp. 538–543.

[40] M. Grant and S. Boyd, "CVX: Matlab software for disciplined convex programming, version 2.2," http://cvxr.com/cvx, Jan. 2020.